Energy & Buildings 348 (2025) 116453

Contents lists available at ScienceDirect

Energy & Buildings

journal homepage: www.elsevier.com/locate/enb

Evaluation of the energy and environmental performance of a novel BIPV window system for net-zero energy buildings

Bo Rang Park [a], A Young Kim [a], Eun Ji Choi [c], Yongseok Jun [b], Jin Woo Moon [a,*]

[a] School of Architecture and Building Science, Chung-Ang University, 84, Heukseok-ro, Dongjak-gu, Seoul 06974, Republic of Korea
[b] Department of Integrative Energy Engineering, Graduate School of Energy and Environment, College of Engineering, Korea University, 145 Anam-ro, Seongbuk-gu, Seoul 02841, Republic of Korea
[c] Postdoctoral Researcher, School of Architecture, University of Southern California, 850 Bloom Walk, Los Angeles, California, USA

ARTICLE INFO

Keywords:
Building-integrated photovoltaic (BIPV)
Smart window
Building energy efficiency
Zero energy building (ZEB)
Net metering
Energy prosumer

ABSTRACT

This study analyzes the indoor environmental performance, energy efficiency, and power generation effects of a horizontal solar strip window (HSSW) employed as a building-integrated photovoltaic system in an elementary school. Using DesignBuilder simulations, the indoor illuminance, indoor temperature, heating and cooling energy demand, lighting energy consumption, power generation capacity, and potential electricity-cost savings are evaluated. The results show that, compared to the reference model employing a low-emissivity window, the HSSW model exhibits a higher annual solar heat gain and indoor temperature, which leads to a lower heating demand and a slight increase in the cooling demand. Due to lower heat loss and higher visible light transmittance, the HSSW model reduces the annual total energy consumption by 1.66%. It also generates 60,575.8 kWh of electricity annually, offsetting the building's total energy use and producing a surplus of 13,460.99 kWh. Employing a net metering scheme with this surplus leads to an annual electricity cost reduction of approximately 1.44 million KRW, illustrating the feasibility of HSSWs as a cost-saving prosumer energy solution. Collectively, these results highlight the potential of HSSWs to contribute to the establishment of net-zero energy buildings and suggest that combining HSSWs with virtual power plants, peer-to-peer energy trading, and energy storage systems may further enhance their economic and energy efficiency.

1. Introduction

1.1. Background and literature review

By 2025, all newly constructed buildings and large-scale renovation projects in the U.S. must meet net-zero energy standards [1]. The U.S. government has also announced a plan to achieve zero carbon emissions for all buildings by 2050. To support this goal, states such as California have introduced programs and incentives that encourage the adoption of renewable energy systems in buildings [2]. New York State, for example, increased its investment in sustainable construction, energy-efficient architecture, and renewable energy deployment to $30 billion in 2024, which has promoted the adoption of net-zero energy buildings (ZEBs) [3]. The European Union (EU) is pursuing similar goals through the Energy Performance of Buildings Directive (EPBD). Under the revised directive published in May 2024 [4], all new buildings must incorporate solar power systems, while renewable energy use in existing buildings continues to expand. This policy aims to transition all EU buildings to zero-carbon status by 2050. This directive also establishes phased renovation targets for underperforming buildings. Member states are required to reduce primary energy consumption in residential buildings by 16 % by 2030 and by 20–22 % by 2035, with at least 55 % of this reduction achieved through renovations targeting the lowest-performing buildings. For non-residential buildings, the directive stipulates that at least 16 % of the least efficient buildings must be renovated by 2030 and 26 % by 2033 to comply with minimum energy performance standards [5].

Similarly, in South Korea, various laws and regulations have been introduced to promote the number of ZEBs. In particular, since 2020, the mandatory implementation of ZEBs has been gradually enforced for public buildings. By 2025, all public buildings must comply with this directive and, by 2030, the regulation will also extend to private

* Corresponding author.
E-mail addresses: pbrighten@cau.ac.kr (B.R. Park), dkdud8936@cau.ac.kr (A. Young Kim), ec_922@usc.edu (E.J. Choi), yongseok@korea.ac.kr (Y. Jun), gilerbert73@cau.ac.kr (J.W. Moon).

https://doi.org/10.1016/j.enbuild.2025.116453
Received 9 April 2025; Received in revised form 4 August 2025; Accepted 14 September 2025
Available online 15 September 2025

buildings. In support of ZEB implementation, several other standards have been introduced, including the Building Energy Efficiency Rating Certification, the mandatory use of renewable energy, and stricter energy-saving design criteria. As of July 2024, the number of certified ZEBs had reached 5,902 [6]. Of these, Grade 5 buildings (defined by an energy self-sufficiency rate of 20–40 %) are the most common, accounting for 3,539 certifications since the introduction of the mandatory policy. In contrast, only 219 Grade 1 buildings, which require an energy self-sufficiency rate of 100 % or higher, have been reported. This illustrates the technical and economic challenges of achieving full energy independence. As regulatory requirements become more stringent and the policy expands to include all buildings, achieving higher energy self-sufficiency rates will become increasingly important.

In order to improve the energy self-sufficiency rate for buildings, there has been a drive to incorporate renewable energy technologies. Doing so not only contributes to the establishment of ZEBs but also allows building owners to generate revenue by selling surplus electricity through power transactions. In South Korea, these transactions can be conducted through power purchase agreements (PPAs) or net-metering via the Korea Electric Power Corporation (KEPCO). In this context, solar power systems are particularly beneficial for power transactions compared to other renewable energy sources for a number of reasons. For example, the global solar power market has been steadily expanding, with the market size expected to reach $377.04 billion by 2030 [7], and government policies that support ZEB certification encourage the use of solar power systems. In addition, solar power systems can be installed on various parts of a building, and recent technological advancements have reduced their installation costs. From a practical perspective, although power generation from solar energy varies with climatic conditions, it remains more predictable and stable than other renewable energy sources.

Recently, as buildings have become larger and taller, it has become increasingly important to secure sufficient space for the installation of photovoltaic (PV) systems in ZEBs. This has led to the emergence of a range of building-integrated photovoltaic (BIPV) designs for rooftops and building facades. However, traditional rooftop PV, building-applied PV (BAPV), and BIPV systems face limitations for high-level ZEB certification due to their limited area. In response, window-type BIPV systems have been proposed and tested as a promising alternative. These units embed semi-transparent solar cell modules into standard window structures, which enables simultaneous daylight transmission, thermal insulation, and electricity generation. The solar cells used in these systems are typically second- and third-generation PV technology. For example, copper indium gallium selenide (CIGS) thin-film cells are a second-generation technology that offers particular advantages for window-type BIPVs, including a thin profile, a simple manufacturing process, flexibility, and adjustable transparency. Though these characteristics preserve daylight penetration and external visibility, the lower efficiency of CIGS cells compared to silicon-based solar cells means that they require a larger surface area to generate sufficient power. To overcome these limitations, third-generation solar cells, such as dye-sensitized solar cells (DSSCs), cadmium telluride (CdTe) cells, and perovskite solar cells, have been developed with a focus on improving cost-effectiveness and performance. Nevertheless, these designs still encounter major issues, including limited efficiency, insufficient durability, long-term instability, scalability problems, inadequate airtight sealing for insulation, toxicity concerns, complex manufacturing processes, and a lack of automation. As a result, full commercialization of these technologies has remained difficult.

Various studies have thus focused on the optimization of window-integrated BIPV systems. For example, Shi et al. (2023) [8] reported that BIPV cladding materials can achieve average building-energy savings of 37.81 % and suggested that PV performance can be improved by focusing on the use of energy-saving materials and building envelopes in electrochromic and photochromic BIPV windows. Their study also suggested that optimizing PV-integrated shading devices (PVSDs), PV double-skin façades, and PV windows is essential for the widespread adoption of efficient BIPV technology. Chung et al. [9] also developed a database using computer simulations to analyze various combinations of the power conversion efficiency (PCE) and visible light transmittance (VLT) for DSSC windows with the aim of identifying optimal performance criteria for ZEBs in small office settings. The results indicated that a VLT of 30 % or higher and a PCE of 13 % (based on the highest PCE reported by NREL in 2020) offered significant energy-saving potential. Furthermore, when the VLT exceeded 50 %, ZEB implementation was found to be achievable across a PCE range of 2 % to 20 %. Similarly, Kim et al. (2020) [10] evaluated the energy generation performance of DSSC windows based on color and transmittance levels. A prototype test was conducted under actual environmental conditions using DSSC windows with various colors and transmittance rates. The results showed that blue DSSC windows, with a transmittance of 7 % and an annual power generation of 14.2 kWh, produced the highest performance.

Research on the energy performance of BIPV window systems has also been actively pursued. Park et al. [11] evaluated the feasibility of solar signage windows fabricated from semi-transparent CdTe solar cells as a building-envelope component. Using simulations, the authors assessed the performance of these windows in four cities across the U.S., with San Francisco demonstrating the highest power generation, achieving annual energy savings of up to 17,970 kWh (105 %). Mohammad et al. [12] also reviewed various types of BIPV window and assessed their energy-saving potential, optimal orientation, and PV technologies when applied to different Köppen climate zones. They found that ventilated double BIPV windows installed facing south exhibited the highest energy-saving potential, thus they represented the most suitable solution for Köppen climate classifications. In another study, Hyun et al. (2022) [13] analyzed the energy consumption of an office building with red and yellow window-integrated DSSCs operated using different lighting-control methods. Their results indicated that the lowest energy consumption occurred when linear/off-lighting control was used in combination with red DSSC windows, with a PCE of 13 % in a small office setting. Chen et al. [14] also developed a set of analytical parameters and a simulation framework to evaluate the impact of BIPV windows installed in street canyon environments. Using an integrated model, the study simulated the energy consumption of buildings with BIPV windows employed in various street canyons during the summer season. The results showed that in Phoenix, U.S., the cooling energy savings ranged from 9.16 % to 63.71 %, with north–south oriented open street canyons and high window-to-wall ratios leading to the greatest reduction in energy consumption.

Recent studies have explored the optimization and energy performance of BIPV technologies across a range of climate conditions and system configurations. For example, Yang et al. [15] investigated the optimal U-value and solar heat gain coefficient (SHGC) for BIPV double-skin façade (BIPV-DSF) systems in three Australian climate zones to enhance thermal comfort and energy efficiency in office buildings. The results identified optimal values of U = 5.16 W/m^{2}K in Darwin, U = 5.87 W/m^{2}K for north-, east-, and west-facing façades in Sydney, and U = 5.16 W/m^{2}K for south-facing façades in both Sydney and Canberra, with the SHGC remaining consistent at 0.81. These findings offer climate-specific design guidelines to improve the performance of BIPV façades. In an earlier study, Yang et al. [16] conducted performance simulations of building-integrated PV/thermal double-skin façades (BIPV/T-DSF) using amorphous silicon, DSSC, and perovskite-based solar cells. The study found that a naturally ventilated, perovskite-based BIPV/T-DSF system yielded the highest energy savings, achieving annual reductions of 34.1 % in Darwin, 86 % in Sydney, and 108 % in Canberra. Their findings confirmed the feasibility of meeting a significant portion of a building's heating and cooling load with electrical and thermal energy harvested from the façade. A subsequent sensitivity analysis by Yang et al. [17] assessed the influence of BIPV/T-DSF design parameters on indoor thermal comfort and energy consumption. The study identified the SHGC of the external window as the most critical factor affecting both outcomes. In other research, Jhumka et al. [18] evaluated the energy performance of various BIPV glazing configurations in Mauritius. The study found that roof-integrated BIPV membranes were more effective in reducing overheating and achieved net energy savings of up to 172 %, while vertically applied BIPV curtain walls increased annual energy consumption by 1.66 %, indicating poor suitability for tropical conditions. In contrast, Roberts et al. [19] analyzed the impact of BIPV-DSFs on daylight availability and energy consumption in office buildings in the UK climate using numerical modeling. A design case with semi-transparent amorphous silicon PV glazing exhibited a 73 % reduction in maximum daylight illuminance compared to a standard DSF. The resulting average and minimum daylight factors (DFs) (0.65 % and 0.00 %, respectively) failed to meet the recommended levels for office environments, while total energy consumption increased by 8 %. These findings suggest that BIPV-DSFs may be unsuitable for commercial installations in the UK climate.

Though this recent research has quantitatively evaluated BIPV performance under various climatic conditions and sought to optimize key façade design parameters such as the double-skin configuration, ventilation type, and glazing properties (e.g., the U-value and SHGC), these studies have tended to focus on office environments and/or façade components rather than on window-integrated systems that simultaneously address visual comfort and power generation. In addition, they have generally lacked integrated evaluations that address the functional requirements of windows, such as the VLT and visual clarity, while there has been little focus on the use of surplus electricity in non-office settings such as educational facilities.

To overcome these limitations, this study proposes a novel horizontal solar strip window (HSSW) that integrates high-efficiency monocrystalline silicon solar cells arranged horizontally across the glazing surface. The cells, cut to dimensions of 155 mm × 85 mm × 0.17 mm, are embedded between a single-glazed pane and an insulated air layer and then combined with an additional glass pane to form a double-glazed structure. This system enables both daylighting and power generation, offering distinct technical and architectural advantages over conventional BIPV windows. This study applied the HSSW system to simulations of an elementary school building and evaluated its impact on the indoor environmental quality, energy consumption, electricity generation, and economic feasibility. A power grid connection scenario was also introduced in which surplus electricity generated by the HSSW exceeded the building's demand. This approach allowed the system to be assessed as a potential energy prosumer model, thus supporting a broader evaluation of its contributions to ZEB implementation and electricity trading.

1.2. Overview of HSSWs

In window-type building-integrated photovoltaics (BIPVs), the use of transparent photovoltaics (TPVs) faces an intrinsic trade-off between visible light transmittance (VLT) and power conversion efficiency (PCE) because a higher VLT is achieved by limiting the absorption of visible light. Traverse et al. [20] highlighted this fundamental limitation by comparing the average visible transmittance (AVT) and PCE of reported TPVs, emphasizing that increased transparency inherently leads to lower photovoltaic efficiency.

The view through a window perceived by the occupant is affected by both direct sunlight and the light reflected from the surrounding environment. In the present study, a transparent PV structure was developed that can utilize the difference between the user's line of sight and the angle of solar incidence. Crystalline silicon solar cells were cut into rectangular shapes, arranged parallel to the occupant's line of sight, and electrically connected to form a module. These bifacial solar cells were employed to utilize most of the light reflected from the surroundings.

The fabricated HSSW was evaluated under vertically incident light using a solar simulator and under natural outdoor sunlight. To improve the performance of the transparent PV, the unit cell size, laser cutting parameters, and modularization conditions were optimized. As a result, the system achieved an AVT of 73.8 %, a color rendering index of 81, and an LSC collection ratio of 59.3 %. Based on these structural and optical characteristics, the TPV system demonstrated the potential to effectively mitigate the transmittance–efficiency trade-off limitation of conventional TPV technologies. In particular, by incorporating the difference between the user's line of sight and the solar incidence angle into the design and employing both bifacial cells and an LSC-based light collection structure, effective visibility and power generation were simultaneously achieved (Fig. 1).

In addition to these structural advantages, the HSSW can be expanded beyond a simple window-type BIPV solution to become a high-value-added architectural feature that integrates display, lighting, and energy production functions. For example, the surface of the solar cells can be combined with LEDs to add information display functions, and high-performance LSC materials can be employed in the spacing between solar cells to achieve state-of-the-art light collection efficiency and a wide range of colors. The supporting substrate can be either glass or a flexible material, and thermal insulation can be provided by combining low-emissivity (Low-E) coatings and electrode technology. Furthermore, a variety of materials (e.g., crystalline silicon, thin films, compound semiconductors, organic and hybrid PVs) can be used, enabling user-customized design in terms of transmittance, color, the color rendering index, and privacy protection. In addition, the proposed HSSW can promote electrical and fire safety by adopting hot spot prevention technology and parallel module configurations that allow for efficient operation even in shaded urban environments.

Accordingly, this study implemented TPV technology in a window-type HSSW system and applied it to an elementary school building, conducting a comprehensive analysis of its effects on the indoor environment and energy performance. This approach provides a technical validation of the functionality of the proposed design as a window, its efficiency as a building system, and its scalability. Ultimately, this study presents evidence that the practical application of highly transparent and efficient window-integrated solar cells can promote the use of BIPV technologies in ZEBs.

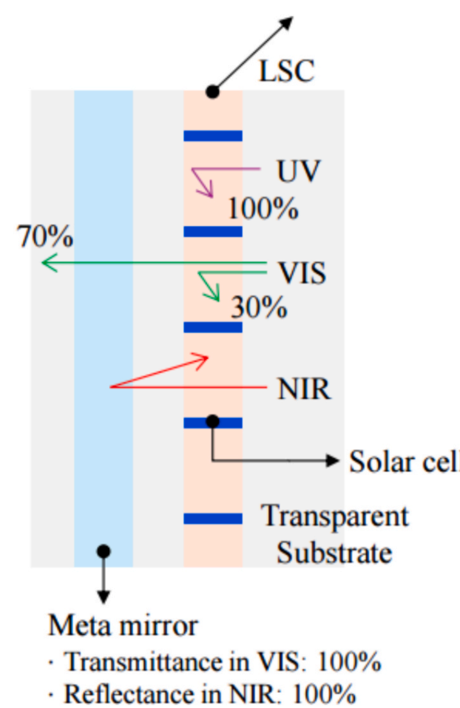

Fig. 1. Configuration and operating principle of the proposed HSSW system. (Abbreviations: LSC – luminescent solar concentrator; UV – ultraviolet radiation; VIS – visible light; NIR – near-infrared radiation).

2. Research scope and method

2.1. Simulation methodology

This study analyzed the feasibility of the proposed HSSW by evaluating its lighting, thermal, and energy performance and its effectiveness for use in ZEBs and energy prosumer applications via the use of surplus electricity. The lighting performance was based on indoor illuminance, which is associated with the VLT of the HSSW, while the thermal analysis considered variation in the indoor temperature resulting from the thermal properties of the HSSW. The energy performance of the system was based on the heating and cooling energy consumption, lighting energy use, and electricity generation capacity. Based on the results of these assessments, the potential of HSSWs to offset building energy consumption through on-site electricity generation and the associated economic benefits for building owners from the sale of surplus power were investigated.

The performance of the HSSW was investigated using computer simulations run on DesignBuilder (Ver. 7.0.2.003) and EnergyPlus (Ver. 9.2.0). DesignBuilder is a comprehensive building-energy simulation software based on EnergyPlus, which incorporates the standard conditions set by LEED and ASHRAE 90.1. The software allows users to input local climate data, building modeling parameters, the thermal insulation properties of the structure, the building operating schedule, HVAC systems, lighting, and internal heat gains. It allows the hourly, monthly, and annual energy consumption, component-specific loads, peak loads, thermal performance, DF, and other key performance indicators to be analyzed [21]. The specific roles and applications of DesignBuilder and EnergyPlus for the present study are illustrated in Fig. 2.

In Korea, the installation of renewable energy systems was mandated in 2008 for educational and research facilities with total floor areas of at least 1,000 m^2 in order to increase the adoption rate of renewable energy [22]. In addition, with the enforcement of mandatory ZEB certification, educational and research facilities with total floor areas exceeding 3,000 m^2 have been required to obtain ZEB certification of at least Grade 5 since 2020 [23]. According to the 2022 Educational Statistics Yearbook published by the Korean Educational Development Institute, the number of elementary, middle, and high schools was 6,175, 3,265, and 2,379, respectively, while the total building-energy consumption, including electricity, gas, and renewable energy, was 280,438 MWh for elementary schools, 136,109 MWh for middle schools, and 131,183 MWh for high schools. Therefore, elementary schools accommodate the largest student population, operate the highest number of schools, and account for the highest energy consumption of the three school levels.

The sources of the energy used in elementary, middle, and high schools in Korea are consistent, with electricity accounting for more than 90 % (including general and nighttime electricity), followed by renewable energy (5 %) and gas (4 %). The 5 % share of renewable energy in elementary schools indicates they have the potential to support the establishment of ZEBs. Compared to residential, office, and commercial facilities, elementary schools have limited operating hours, operating primarily during the daytime. In addition, the shape of school buildings is relatively simple with a large roof area, a high window-to-wall ratio (20–40 %), and low variation in room usage, which makes them ideal for maximizing energy savings and integrating renewable energy sources. If adequately implemented, elementary schools could serve as a successful model for ZEBs. Furthermore, elementary schools are distributed nationwide, and their transition to ZEBs could provide pleasant learning environment and improve health conditions for students [24]. Therefore, this study focused on elementary school buildings as the site for the proposed HSSW, with the aim of evaluating the indoor environmental conditions, building energy consumption, and power generation capacity. Based on this analysis, this study assessed the feasibility of establishing ZEBs and examined the potential for energy prosumer applications.

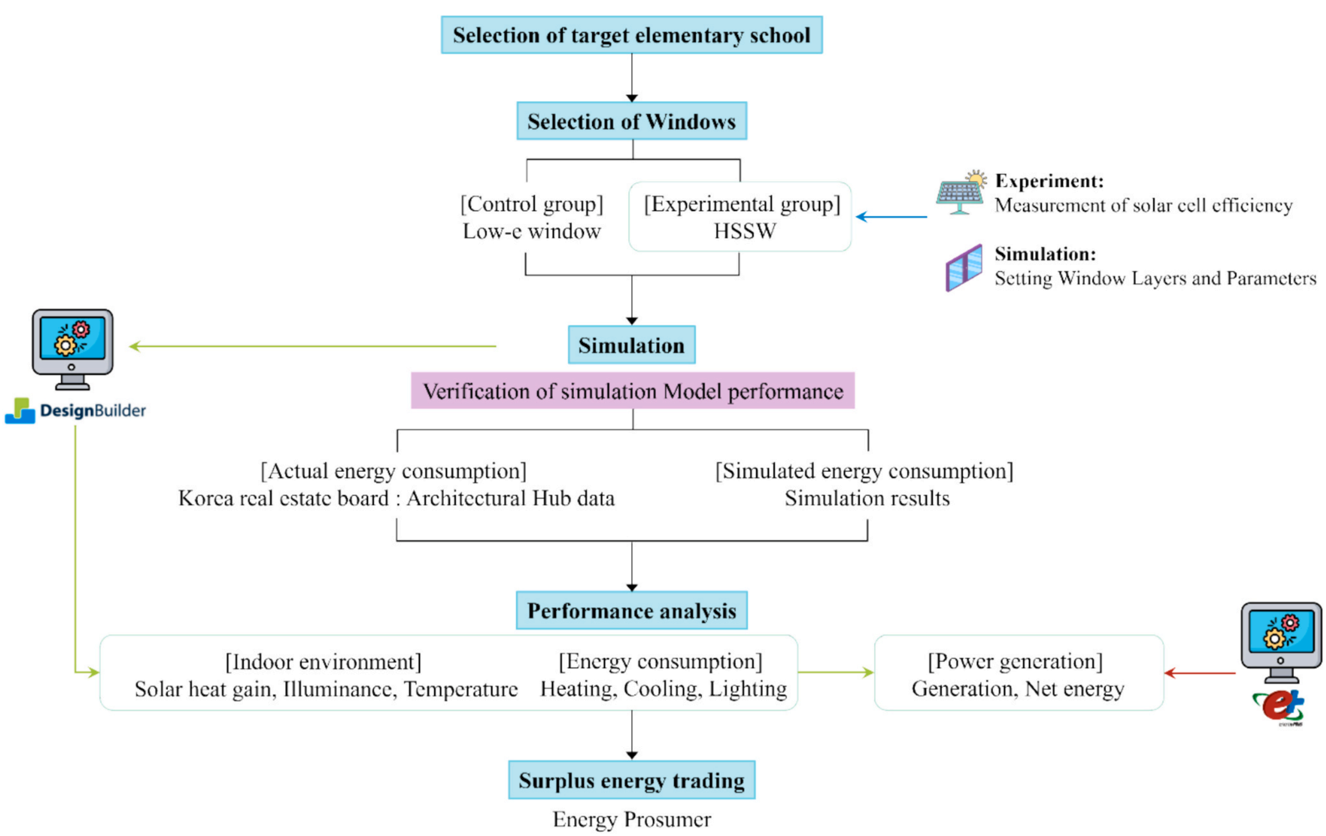

Fig. 2. Flowchart illustrating the research methodology used in the present study.

2.2. Building modeling

The target elementary school was designed based on previous studies, with a standard scale and detailed physical properties defined accordingly [25,26]. The climate zone was set to Seoul, South Korea, with a south-facing orientation and a rectangular double-corridor layout. The building had a total floor area of 5,513 m^2 and five stories. An overview of the building configuration and detailed specifications are provided in Fig. 3 and Table 1, respectively.

The building space was divided into conditioned and unconditioned zones. The conditioned spaces included general classrooms, special classrooms 1 and 2, and the teachers' office, while the unconditioned spaces consisted of stairwells, other common areas, and core spaces. The window-to-wall ratio was set to 27.6 %, which falls within the typical range of 20–40 % for elementary schools. To maximize PV power generation, HSSWs were installed for the south, east, and west-facing windows, taking into account solar irradiance, which directly affects electricity production. The north-facing windows were fitted with Low-E windows instead of PV-integrated glazing.

2.3. HSSW modeling

The indoor environmental performance and energy consumption of the proposed HSSW design were compared with those of Low-E windows, which are widely used in buildings in Korea. Specifications for these two window types are provided in Table 2. The HSSW was a double-glazed window composed of a PV-integrated single-pane glass unit, an argon-filled layer, and a clear glass layer (PV glass: 24 mm; Ar: 13 mm; clear glass: 3 mm). The PV-integrated component consisted of horizontally layered solar cells (HLSCs) (Fig. 4) manufactured using monocrystalline silicon solar cells provided by company "L." These solar cells were cut to dimensions of 155 mm (W) × 10 mm (D) × 0.17 mm (H) and horizontally arranged with a 7.5 mm spacing. The gaps between the PV cells were filled with a polydimethylsiloxane (PDMS)-based silicone epoxy resin, forming a laminated single-pane glass structure.

The thermal and optical performance of the HLSC unit within the proposed HSSW is presented in Table 3, based on test results from Korea Conformity Laboratories (KCL). The tests followed KS L 2514:2011, NFRC 300:2023, and KS L 2525:2006 standards, covering the 14 parameters listed in Table 3. The thermal resistance was calculated using KS L 9016:2010, while the power generation efficiency was determined based on in-house experiments conducted by the HLSC manufacturer. Fig. 5 presents the test HSSW samples used (100 mm × 100 mm and 300 mm × 300 mm) for the thermal resistance testing of the silicone-based filler.

The data obtained from the tests were used in combination with International Glazing Database (IGDB) and WINDOW 6 data to define the glass properties in DesignBuilder. Based on this configuration, the U-value, SHGC, and VLT of the HSSW were determined. For the Low-E window, the material properties were defined using certified product data from the glass manufacturer.

3. Results and discussion

3.1. Validation of the simulation

The simulation model used in the present study was developed based on the Korean Building Energy Efficiency Design Standards and relevant prior research. To ensure the reliability of the simulation results, model validation was conducted in accordance with ASHRAE Guideline 14. For this purpose, reference data provided by Architecture HUB were utilized [27]. Architecture HUB is an integrated information system that provides a wide range of data related to architecture and the building service industry in South Korea. To validate the reliability of the simulation model for the present study, electricity consumption data were collected from 50 buildings that were similar in terms of location, year of completion, structure, usage, and number of floors. The collected data were converted into energy consumption per unit area and analyzed using the energy use intensity (EUI), which is calculated by dividing the annual energy consumption by the total floor area of a building (unit: kWh/m^2·yr). A box plot was used to visualize the variability in the EUI results for the sample data and the simulation output based on the median and interquartile range (IQR). In this comparison, the average EUI error, coefficient of variation of the root mean square error (CV (RMSE)), and mean absolute error (MAE) were used as the key metrics. The simulation model used for validation was configured with a standard Low-E window, and lighting control features were excluded from analysis.

As shown in Fig. 6, the EUI of the 50 sample buildings ranged from a minimum of 14.44 kWh/m^2·yr to a maximum of 54.07 kWh/m^2·yr, with an average of 30.06 kWh/m^2·yr. The simulation result was calculated to be 32.12 kWh/m^2·yr based on a total floor area of 5,512.5 m^2 and an annual energy consumption of 117,049.8 kWh/yr. Table 4 presents the degree of accordance between the sample data and the simulation model. The average EUI error was 6.85 %, with a CV(RMSE) of 6.12 % and an MAE of 2.06 %, all of which satisfy the allowable thresholds

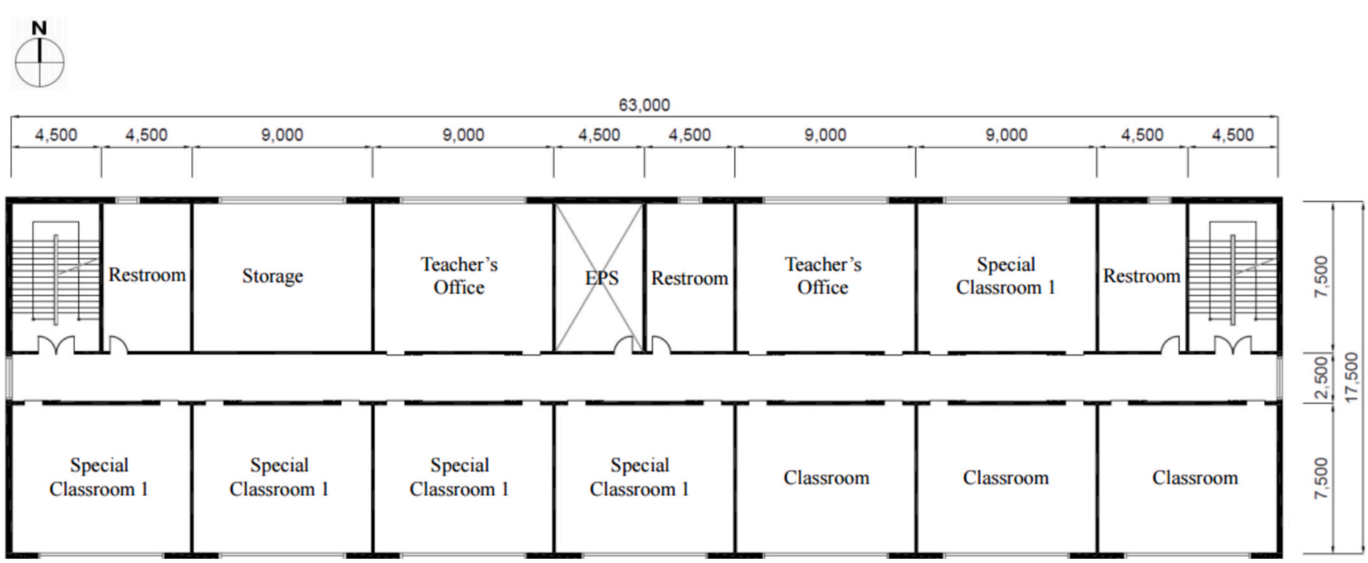

Fig. 3. Floor plan of the modeled elementary school.

Table 1
Key parameters used to model the building.

(a) Schedules

Item	Type	
Vacation periods	Summer	July 27 to August 23
	Winter	December 31 to February 28
Heating and cooling periods (excluding vacation)	Heating	January 1 to April 30, October 1 to December 31
	Cooling	May 1 to September 30

(b) Overview of the space and equipment density

Space		No. of Rooms	Area [m^2]	Equipment [W/m^2]	Occupancy [m^2/person]	Operating period
Air-conditioned	Classroom	20	67.50	2	0.37	Semester
	Special classroom 1	16	67.50	2	0.37	Semester
	Special classroom 2	7	67.50	30	0.37	Semester
	Teacher's office	6	67.50	12	0.53	Semester
	Stair	10	33.75	–	–	Annual
Non-air-conditioned	Restroom	15	33.75	–	–	Annual
	Corridor	5	157.50	–	–	Annual
	EPS	5	33.75	10	–	Annual
	Storage	4	67.50	–	–	–
	Electrical	1	67.50	50	–	Annual

(c) General information

Item	Parameter		Value
Building structure	Location		Republic of Korea, Seoul
	Type		Elementary school
	Total floor area		5,512.5 m^2 (1,102.5 m^2 for each floor)
	Number of floors		5
	Floor to floor		4.6 *m*
	Floor to ceiling		3.6 *m*
	Wall-to-wall ratio		27.6%
Construction materials (U-values)	Exterior wall		0.15 W/m^{2}K
	Roof		0.24 W/m^{2}K
	Ground floor		0.29 W/m^{2}K
	Window	Low-E	1.54 W/m^{2}K
		HSSW	1.50 W/m^{2}K
Occupied load	Lighting	Conditioned area	10 W/m^2
		Non-conditioned area	4 W/m^2
	People	Classroom	0.37 m^2/person
		Special classroom	0.37 m^2/person
		Teacher's office	0.53 m^2/person
	Office equipment	Classroom	2 W/m^2
		Special classroom	2 W/m^2
		Teacher's office	12 W/m^2
		EPS	10 W/m^2
		Electrical room	50 W/m^2
	Dimming control		
Heating/cooling –system	Fan coil unit	4 pipes	
	Fuel	Electricity for grid	
	COP	Heating 4.0 / Cooling 4.2	
	Set-point temperature	Heating 20℃ / Cooling 26℃	
	Set-back temperature	Heating 15.5℃ / Cooling 29.4℃	
DHW system	Instantaneous	0.95 / Electricity	

Table 2
Physical properties of the exterior window.

Type	Glazing layer [No. thickness, mm]	U-value [W/m^{2}K]	SHGC	VLT [%]	Eff [%]	Note
Low-E	Clr 6 + Air 12 + Clr 6	1.54	0.57	74.50	–	Baseline
HSSW	HLSC 24 + Arg 13 + Clr 3	1.50	0.73	81.40	20.52	–

specified in ASHRAE Guideline 14 [28,29] (CV(RMSE) ≤ 15 % and MAE ≤ 5 kWh/m^2·yr). Therefore, the simulation model constructed in the present study can be regarded as a highly reliable analytical tool.

3.2. Indoor environment

The effect of the HSSW system on the indoor environment was analyzed based on the lighting and thermal performance. Lighting performance was assessed using two indicators: the DF, which evaluates static natural daylighting performance, and illuminance, which represents the absolute quantity of light. The simulation space for the indoor illuminance analysis was a classroom located at the center of the south-

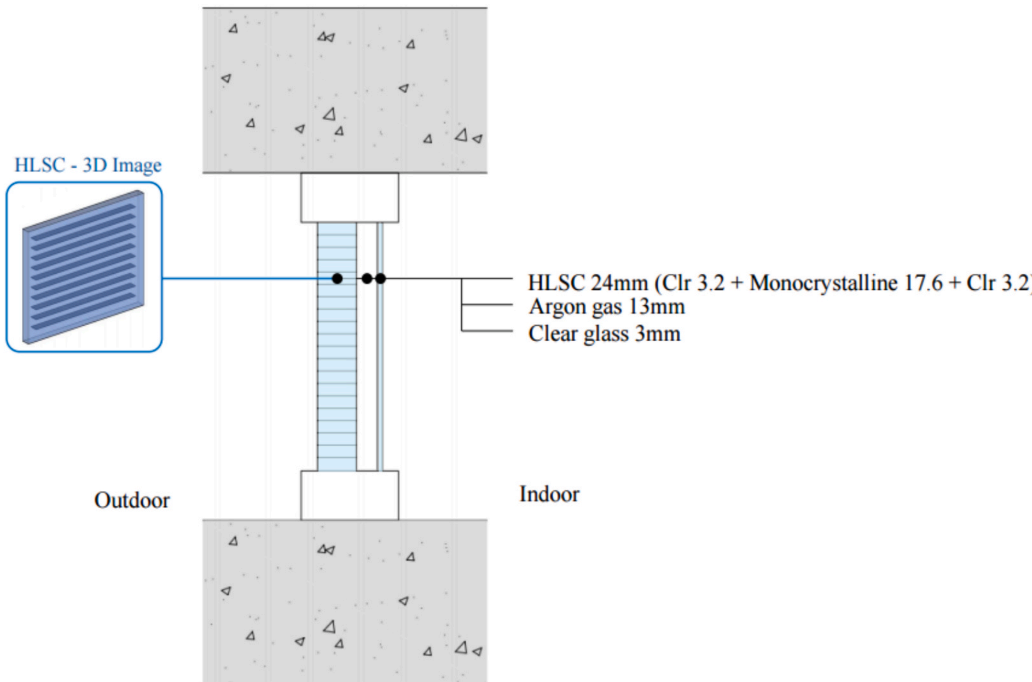

Fig. 4. Cross-section of the HSSW used in this study.

Table 3
Physical properties of the HLSC units.

Property	Value
Thickness [mm]	24.00
U-value [W/m^{2}K]	3.83
Solar heat gain coefficient	0.80
Visible transmittance [%]	90.00
Inside visible reflectance [%]	8.00
Outside visible reflectance [%]	7.90
Solar transmittance [%]	73.30
Inside solar reflectance [%]	7.10
Outside solar reflectance [%]	7.00
Infrared transmittance [%]	56.90
Inside infrared reflectance [%]	6.20
Outside infrared reflectance [%]	6.10
Shading coefficient	0.91
Emissivity [%]	0.84
Efficiency [%]	20.52

Fig. 5. Photographs of the HSSWs used for testing.

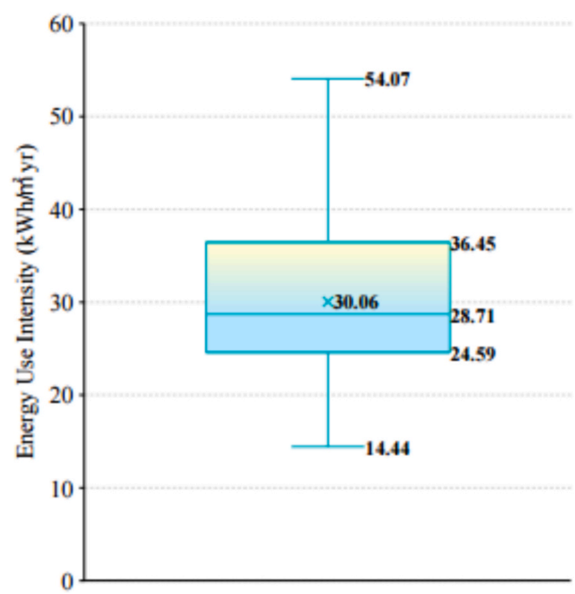

Fig. 6. Energy use intensity (EUI) results derived from the simulation.

Table 4
Summary of the reliability analysis for the simulation model, including the EUI error, CV(RMSE), and MAE based on ASHRAE Guideline 14.

Model	EUI [kWh/m^{2}yr]	EUI error [%]	CV(RMSE) [%]	MAE [kWh/m^{2}yr]
Sample (baseline)	Aver. 30.06	–	–	–
Simulation	32.12	6.85	6.12	2.06

facing side on the third floor, which is located in the middle level of the elementary school. The reference space had dimensions of 8.84 m (W) × 7.10 m (D). A daylighting sensor was positioned at the center of the room at a height of 0.8 m, corresponding to the working plane level. The analysis assumed an overcast sky, and the date and time were set to December 22 at 12:00 PM based on previous studies [30] because this corresponds to the peak average illuminance from a south-facing window under overcast conditions.

Though there is no clearly defined standard value for the DF, the

Leadership in Energy and Environmental Design (LEED) certification requires a minimum DF of 2 %. Hence, a range of 2–5 % is generally considered appropriate. For indoor illuminance, in South Korea, the Korean Industrial Standards (KS) specify an average illuminance of 400 lx for classrooms. Internationally, the Chartered Institute of Building Services Engineers (CIBSE) and the International Commission on Illumination (CIE) recommend an average illuminance of 300 lx, while the Illuminating Engineering Society (IES) suggests 700 lx as suitable indoor illuminance for learning and writing activities.

As shown in Table 5, the average DF of the elementary school obtained from the simulation was 3.5 % for the Low-E windows and 3.9 % for HSSWs, meaning that both window types exceeded the recommended minimum LEED DF standard (>2%). Similarly, the average indoor illuminance was 1,025.5 lx for HSSW and 933.6 lx for Low-E windows, thus both met the recommended standards. The indoor illuminance of HSSW was 8.9 % higher than that of the reference model due to the higher VLT. However, the minimum illuminance recorded was 32 lx (Fig. 7) at a distance of approximately 3.5 m from the classroom window, thus natural daylight alone was insufficient to meet the 300 lx classroom illuminance standard. This suggests that, in addition to natural daylighting, an appropriately designed artificial lighting system is necessary to ensure visual comfort for the occupants.

The thermal performance analysis of the two window types focused on the variation in the indoor temperature. The target space was the same third-floor center classroom as used for the lighting performance analysis. The indoor temperature was assessed based on the solar heat gain, which represents the actual amount of solar energy entering the room through the window and is closely linked to heating and cooling loads. This was calculated using the SHGC, incident solar radiation energy, and the window surface area. The SHGC is defined as the proportion of solar radiation transmitted into the indoor space and expressed as a value between 0 and 1. A higher SHGC results in greater heat gain at the same solar radiation level. To isolate the effect of the window performance on the indoor temperature, the HVAC system was turned off during the simulation.

As shown in Fig. 8, the annual solar heat gain through the windows was approximately 36.46 % higher for the HSSWs than for the Low-E windows. This trend was in line with the SHGC, which was 0.73 for the HSSWs and 0.57 for the Low-E windows, a difference of 21.92 %. Both window types exhibited the highest solar heat gain in January and February, when the solar altitude was lower, whereas the lowest solar heat gain was observed in July and August, when the solar altitude was higher. Furthermore, during winter, when the solar heat gain was higher, the difference between the two window types was more pronounced.

Fig. 9 illustrates the monthly changes in the indoor temperature for both window types. During the summer months (May to September), the average indoor temperature was 23.4 °C for the Low-E windows and 27.5 °C for HSSWs. Similarly, during the winter months (October to March), the six-month average indoor temperature was about 1.3 °C higher for the HSSWs than for the reference model. The temperature difference was more pronounced in winter because the HSSWs had a higher SHGC and greater solar heat gain in this season compared to the Low-E windows. In addition, the U-value of the HSSWs was slightly better than that of the reference model, which also increased the indoor temperature. These findings suggest that using HSSWs can reduce the heating demand compared to the reference model, while the cooling demand may slightly increase.

Table 5
DF and indoor illuminance of both window types for the simulated elementary school conditions.

Window type	DF [%]			Illuminance [lux]		
	Min.	Max.	Aver.	Min.	Max.	Aver.
Low-E (baseline)	0.3	18.3	3.5	28.97	1,838.3	933.6
HSSW	0.3	20.0	3.9	32.0	2,016.9	1,025.5

3.3. Energy consumption

To analyze the impact of HSSWs on the building energy consumption, the use of energy for heating, cooling, and lighting was evaluated. The net energy consumption of the HSSWs was also assessed by incorporating electricity generation from PV. Figs. 10 and 11 and Table 6 show the monthly and annual data for heating, cooling, and lighting energy consumption. The total energy consumption for HSSWs was 47,114.81 kWh/yr, which was 1.66 % lower than for the reference model.

The annual heating energy consumption for HSSW (19,624.29 kWh/yr) was 11.65 % lower than that of the reference model. This can be attributed to the superior thermal transmittance of the HSSWs (as indicated by the U-value), which reduced indoor heat loss during winter compared to the Low-E windows. During the heating period (excluding the vacation months January and February and non-heating months May to September), December and March experienced the highest heating energy consumption due to the low average outdoor temperature. The difference in heating energy consumption between the HSSWs and the Low-E windows was greater when the outdoor temperatures were lower.

Conversely, the annual cooling-energy consumption was 11,057.57 kWh/yr for the reference model, which was 21.39 % lower than for the HSSWs. The increased cooling energy demand for the HSSWs was likely due to difficulties in dissipating internal heat during summer because of their effective insulation and airtightness. In addition, the higher VLT performance increased the lighting-induced heat gain, and higher SHGC values resulted in overcooling. During the cooling period, September experienced the largest difference in energy consumption. This is likely because the annual solar radiation levels were highest and the indoor temperatures increased during this month. Based on these findings, HSSWs are expected to be particularly effective in reducing heating energy consumption in cold climates, where buildings are typically more vulnerable to indoor heat loss.

Lighting control was also implemented to analyze the impact of VLT on the lighting energy consumption for each window type. The lighting control method was selected from the built-in options in DesignBuilder, which included linear, stepped, and linear/off. Of these, the linear method, which adjusts the lighting output proportionally to variation in natural daylight, was employed because it allows for a more precise analysis of changes in lighting energy consumption. The resulting simulations also closely resemble real-life lighting usage conditions. The target illuminance levels for the control were set to 400 lx for the classrooms and 200 lx for the core spaces. The control sensors were configured with the same environmental settings as those used for the indoor illuminance analysis for different VLT values.

The annual lighting-energy consumption was 3.83 % (560.83 kWh/yr) higher for the reference model than for the HSSWs. This could be attributed to differences in the VLT, which was 74.5 % for the Low-E windows and 81.4 % for the HSSWs, representing a 9 % difference. This led to the greater use of artificial lighting in the room with Low-E windows. In addition, indoor illuminance, which directly affects lighting energy consumption, is generally more impacted by direct solar radiation than by diffuse radiation because the former leads to stronger illumination. As shown in Fig. 8, direct solar radiation was higher in winter than in summer, which was in accordance with the findings that the lighting-energy consumption was also higher in winter (excluding the vacation period).

Power generation was analyzed based on the installation area of the HSSWs and their orientation (Tables 7 and 8; Figs. 12 and 13) and subsequently evaluated in terms of the net energy performance. In the modeled elementary school, the HSSWs were installed in the south-, east-, and west-facing facades, while the north-facing windows were not equipped with PVs. The installation area was 412.34 m^2 on the south

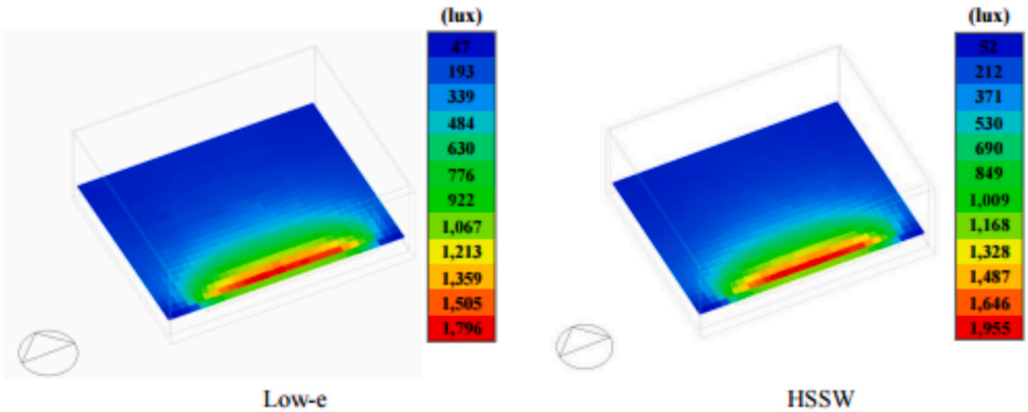

Fig. 7. Indoor illuminance for the two window types, measured along the horizontal plane at 0.2 m grid intervals.

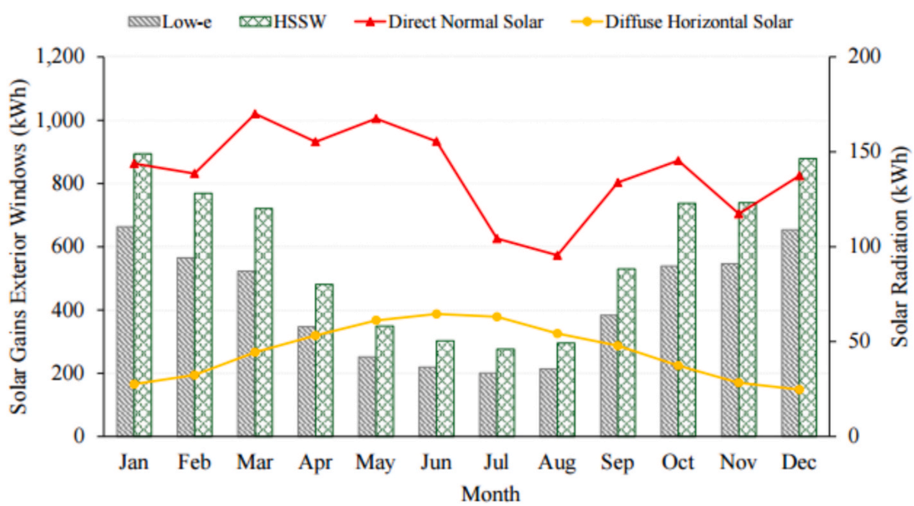

Fig. 8. Solar heat gain for the two window types during the year.

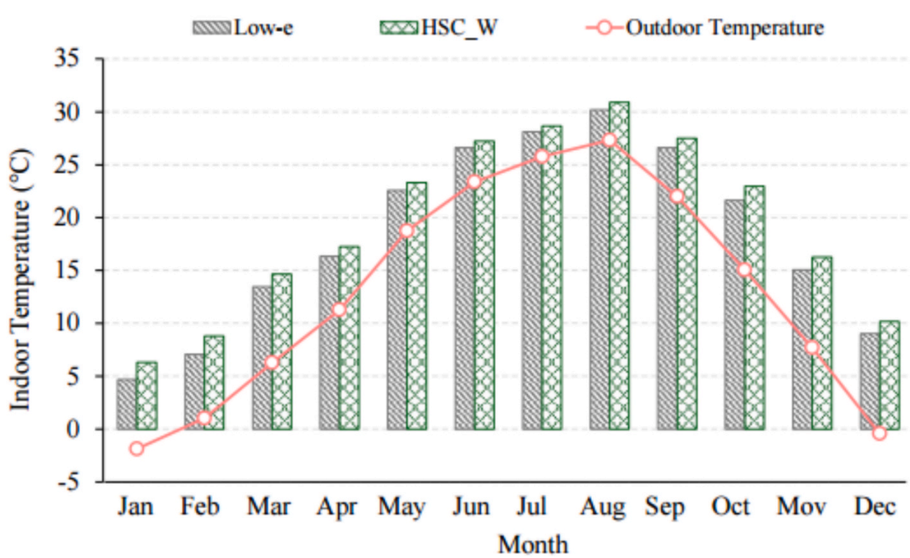

Fig. 9. Indoor temperature for the two window types throughout the year.

side and 33.05 m^2 on each of the east and west-facing walls, while the net PV cell area was 412.34 m^2 on the south side and 20.46 m^2 on each of the east and west sides. With a PV capacity of 135 W/m^2, the total installed capacity for the target building was 61.19 kW. Due to the classroom layout and façade window design, the south-facing HSSWs accounted for 89 % of the total window area.

In terms of the annual power generation from the HSSWs, the south-facing windows produced the highest output at 55,747.2 kWh/yr, while

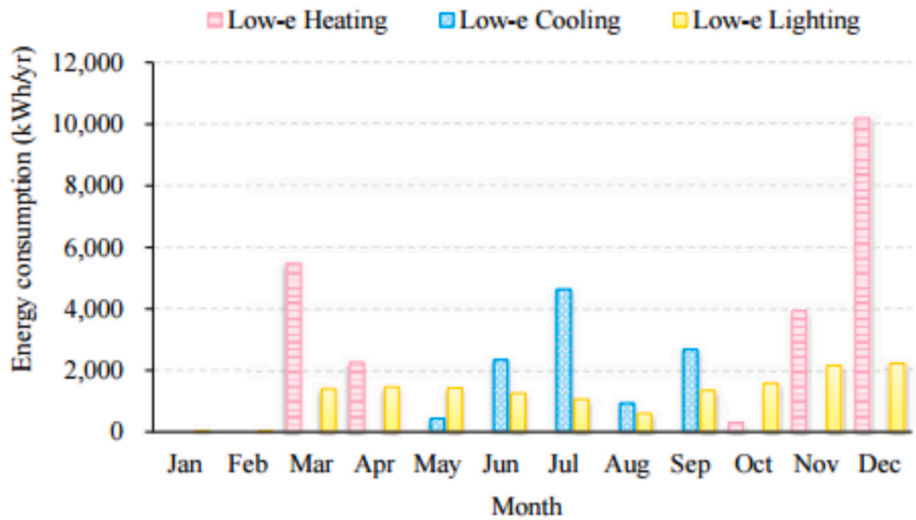

Fig. 10. Monthly energy consumption of the reference model (Low-E windows) throughout the year.

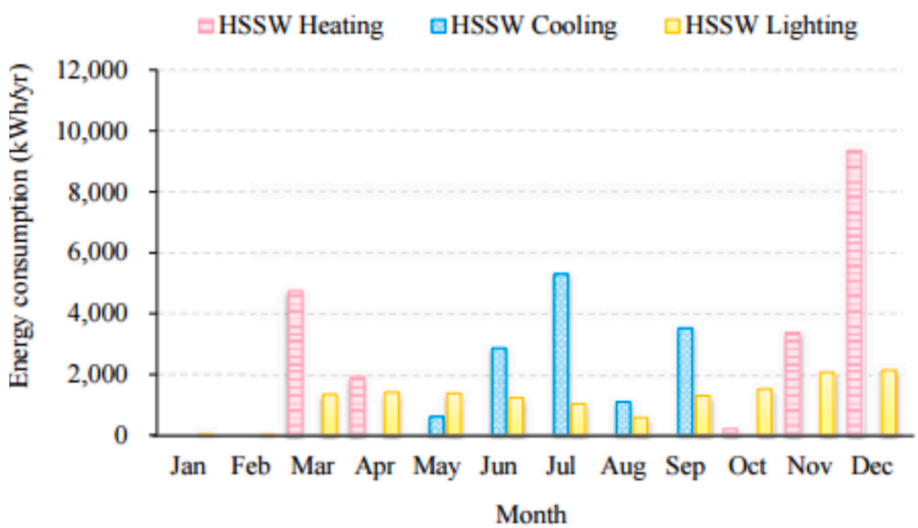

Fig. 11. Monthly energy consumption of the HSSWs throughout the year.

Table 6
Annual energy consumption for both window types.

Type	Annual energy usage [kWh/yr]			
	Heating	Cooling	Lighting	Total
Low-E	22,211.59	11,057.57	14,628.18	47,897.34
HSSW	19,624.29	13,423.18	14,067.34	47,114.81

Table 7
Window count, window area, and PV area for the different window orientations.

Type	No. of windows	Window area [m^2]	PV area [m^2]	Generation [kWh/yr]
South	35	417.73	412.34	55,747.7
East	5	33.05	20.46	2,525.2
West	5	33.05	20.46	2,302.8

the east- and west-facing HSSWs generated 2,525.2 kWh/yr and 2,302.8 kWh/yr, respectively. As shown in Fig. 12, the power generation of the south-facing HSSWs was closely associated with the direct solar radiation, which is naturally the highest for south-facing façades in the Northern Hemisphere. In contrast, the power generation trends for the east- and west-facing HSSWs were more closely associated with variation in the diffuse solar radiation because their exposure to direct sunlight was limited to the morning and afternoon, respectively. This leads to a higher fraction of diffuse solar radiation, which has no specific directionality.

Table 8
Annual net-energy consumption and power generation of the two window types.

Type	Annual energy [kWh/yr]	
	Power generation	Net energy
Low-E	–	47,897.34
HSSW	60,575.80	–13,460.99

The higher PV generation observed in March and October (spring and autumn, respectively) for the south-facing HSSWs was attributed to a combination of climatic and technical factors. In Seoul, these months are typically characterized by clear skies with low atmospheric moisture and particulate concentrations, resulting in higher levels of direct solar radiation (see Fig. 8). During these periods, solar radiation strikes the vertical façade at angles that are nearly perpendicular, meaning that the

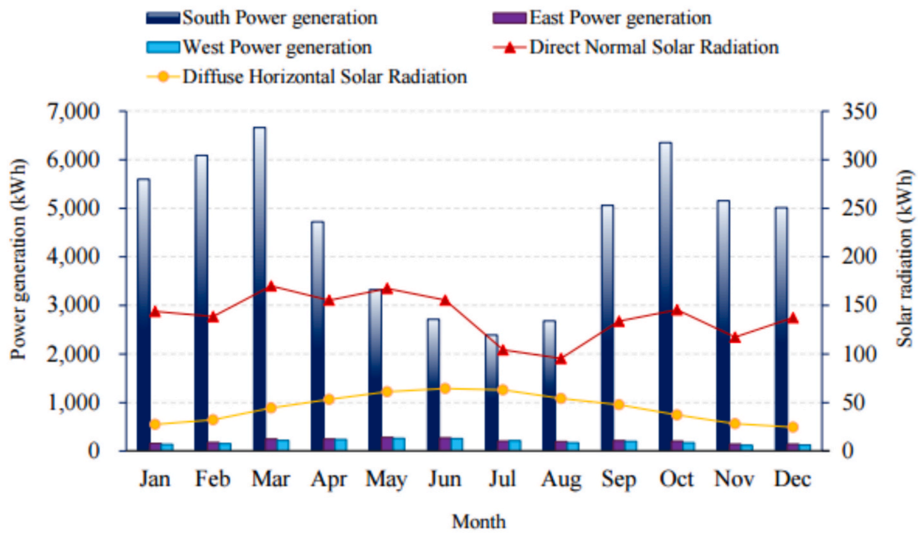

Fig. 12. Monthly power generation of the HSSWs according to their orientation.

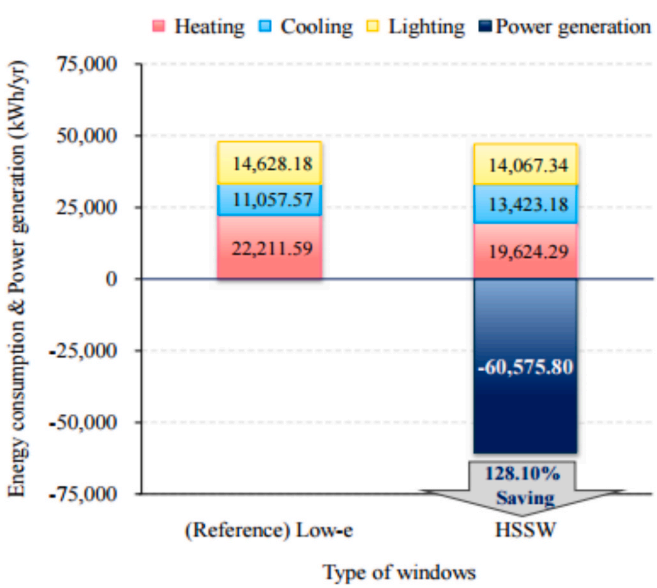

Fig. 13. Annual total energy consumption and power generation for the two window types.

horizontally arranged HSSW modules receive optimal levels of direct irradiance. In contrast, during summer, the higher solar altitude leads to steeper angles of incidence on the horizontal modules, which is less favorable for power generation. Additionally, higher humidity and frequent cloud cover during summer contribute to a higher proportion of diffuse radiation, reducing the conversion efficiency. Another explanation is that, because PV modules are sensitive to temperature, the cooler ambient conditions in March and October help maintain lower module surface temperatures. This avoids thermal degradation and allows the modules to operate at optimal efficiency. Conversely, the higher outdoor temperatures during summer raise the module temperature, which negatively affects the PCE.

Compared to the south-facing HSSWs, the east- and west-facing systems delivered more stable power output on cloudy days, with less variation between sunny and overcast conditions. In addition, their power generation was higher in summer than in winter because the sunlight undergoes more Raleigh scattering as the solar altitude increases, which disperses radiation in all directions. At the same time, higher humidity levels increase the number of atmospheric particles, which increases Raleigh scattering and diffuse radiation further. The east-facing HSSWs produced slightly more power than the west-facing HSSWs. This difference can be attributed to higher air quality in the morning when the east-facing panels receive sunlight, while air pollution and fine dust levels increase in the afternoon and reduce the efficiency of the west-facing panels. Moreover, solar panels generally operate more efficiently at lower temperatures. Because morning temperatures are typically lower than afternoon temperatures, east-facing panels tend to generate more power. Therefore, prioritizing east-facing facades over west-facing facades when installing solar panels may lead to higher overall power generation efficiency.

The annual total power generation from the HSSW installation was 60,575.8 kWh, which fully covered the total energy consumption of 47,114.81 kWh/yr and produced a surplus of 13,460.99 kWh/yr. This indicates that ZEB implementation was feasible. In addition, the surplus electricity could be used to generate additional revenue through the net metering system offered by KEPCO.

3.4. Energy performance according to the climate conditions

To quantitatively evaluate the sensitivity of the HSSW system to the climate, the influence of the sky conditions on PV power generation and building energy consumption was analyzed. In this analysis, the hourly sky conditions were classified into clear, intermediate, and overcast using the annual weather data (EPW). The criteria used for this classification followed the Perez Sky Model [31], which is commonly employed in simulation tools such as EnergyPlus and Radiance (Table 9).

Representative days were then selected for each sky condition in each season. To achieve this, the days satisfying the respective sky condition criteria were first identified for each season, and then the day with a global horizontal irradiance—calculated as the sum of the direct normal irradiance (DNI) and diffuse horizontal irradiance (DHI)—closest to the seasonal average was chosen (see Table 9 for a list of these

Table 9
Classification criteria for sky conditions based on the Perez model.

Sky conditions	DNI [W/m^2]	DHI [W/m^2]	Representative dates
Clear	≥600	≤100	Mar. 8, Nov. 3, Dec. 19
Intermediate	200—600	100–300	Feb. 3, Apr. 13, Jul. 25, Sep. 23
Overcast	≤200	≥300	May 12, Jul. 18, Sep. 12

(Abbreviation: DNI – direct normal irradiance; DHI – diffuse horizontal irradiance).

days). The seasons were defined as spring (March–May), summer (June–August), autumn (September–November), and winter (December–February). Using these representative days, PV generation and the energy consumption for cooling, heating, and lighting were analyzed.

According to the analysis of DNI and DHI data for Seoul, intermediate sky conditions were most frequently observed throughout the year, followed by clear and overcast conditions. Seasonally, clear skies were most common in winter, overcast skies were predominantly observed in summer, while spring and autumn were largely characterized by intermediate skies. These results reflecting the unique seasonal characteristics of the Seoul climate.

The energy consumption and PV generation varied according to these sky conditions (Fig. 14). Under clear skies, heating demand peaked at 1,667.3 kWh, while lighting demand and PV generation were both 7.82 kWh. This was attributed to the low outdoor temperatures in winter, which increased the heating load, and the reduced lighting use due to low occupancy during the winter break (December 31–February 28). Additionally, despite high solar irradiance in December, the short daylight hours limited PV generation. Under intermediate skies, the cooling demand was highest at 1,645.2 kWh, with lighting consumption at 118.87 kWh and PV generation at 7.03 kWh. This was primarily due to the inclusion of representative days from the academic summer session (e.g., July 25) and early autumn (e.g., September 23), when cooling needs are higher. Intermediate skies are associated with a mix of direct and diffuse irradiance, leading to stable PV performance, but the simultaneous demand for cooling and lighting disrupted the net energy balance. Overcast skies led to the highest lighting load at 148.7 kWh and a cooling load of 537.8 kWh, while PV generation dropped to 2.78 kWh. These results reflect typical overcast conditions during the rainy season or humid summer weather, characterized by limited daylight penetration, increased reliance on artificial lighting, and the need for air conditioning to maintain indoor comfort.

Overall, these results demonstrated that the climate conditions had a varying effect on the net energy balance of the modeled classroom. For example, the heating demand was found to be most sensitive to clear skies. Though direct solar irradiance was present, its contribution to heating was limited because the low outdoor temperatures played a dominant role, significantly increasing the heating load. Under intermediate sky conditions, cooling demand exhibited the highest sensitivity. During transitional seasons such as spring and autumn, cooling loads rose rapidly. While the PV output remained relatively stable, the simultaneous increase in both cooling and lighting demands had a negative impact on the net energy balance. For overcast sky conditions, a strong inverse correlation between lighting demand and PV generation was observed. Reduced solar irradiance significantly reduced PV output, whereas the lighting energy demand increased sharply, leading to the most unfavorable overall energy balance.

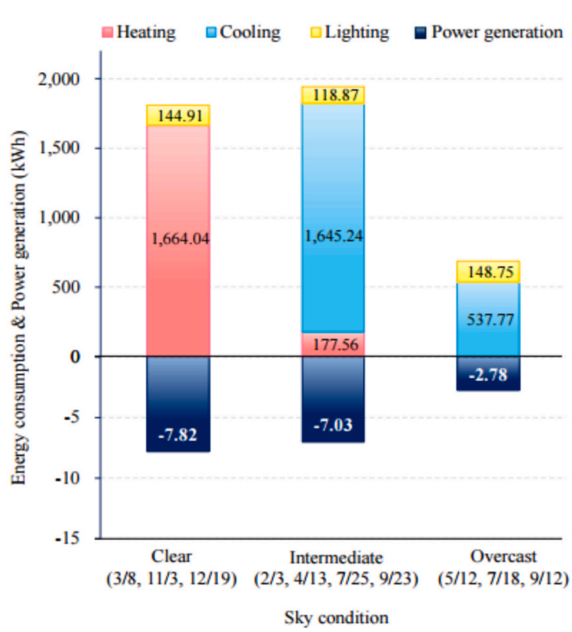

Fig. 14. Energy use and PV generation of the HSSWs according to the sky conditions.

These findings offer important implications for the design and operation of ZEBs. During winter, when clear skies are predominant, improving envelope insulation and heating system efficiency is critical to reducing the heating load. For intermediate conditions, increasing PV output through high-efficiency BIPVs or the addition of energy storage systems is necessary to offset cooling demands. Under overcast skies, optimizing daylighting systems and deploying advanced lighting controls are required. Additionally, the operational characteristics of elementary schools—such as the reduced occupancy during vacation periods—should be considered in the design of lighting and HVAC control strategies to enhance energy efficiency.

3.5. Evaluation of the energy prosumer potential

This study examined the electricity cost savings achievable when surplus electricity generated by the HSSWs after meeting the building's energy needs was used in the net metering system run by KEPCO [32]. In the net metering system, customers can supply surplus electricity to KEPCO and offset it against the electricity they consume from the grid. This program applies to renewable energy systems with a capacity of up to 10 kW, except for solar energy systems, which have an allowable capacity of up to 1,000 kW, provided that they are installed at the same location as the electricity usage.

Because the modeled building was an elementary school, our analysis applied the Educational Power Supply (Type A) I rate provided by KEPCO. This rate varies by season, with a basic charge added based on the contracted power capacity. For the present study, only the electricity usage charges were calculated. The seasonal electricity rates were 116.2 KRW/kWh for summer (June to August), 95.4 KRW/kWh for spring and autumn (March to May and September to October, respectively), and 114.5 KRW/kWh for winter (November to February). Using the monthly energy consumption of the HSSWs (see Figs. 9 and 10), the monthly electricity charges were calculated using Eq. (1), and the results are presented in Table 10.

Table 10
Electricity costs based on the monthly energy consumption for different seasonal plans.

Month	Energy consumption [kWh]	Seasonal plan	Electricity rate [KRW/kWh]	Monthly electricity cost [KRW]
Jan.	44.39	Winter	114.5	5,084
Feb.	36.40	Winter	114.5	4,169
Mar.	6,096.44	Spring & Fall	94.4	575,523
Apr.	3,336.96	Spring & Fall	94.4	314,944
May	1,998.83	Spring & Fall	94.4	188,727
Jun.	4,097.07	Summer	116.2	476,059
Jul.	6,330.87	Summer	116.2	735,587
Aug.	1,684.38	Summer	116.2	195,789
Sep.	4,826.90	Spring & Fall	94.4	455,611
Oct.	1,724.92	Spring & Fall	94.4	162,824
Nov.	5,444.32	Winter	114.5	623,401
Dec.	11,493.07	Winter	114.5	1,315,975
Total	47,118.80	–	–	5,053,693

$$Monthlyelectricitycost(KRW) = monthlyenergyconsumption \times monthlyelectricityrate \quad (1)$$

The annual total energy consumption for the target building was 47,114.8 kWh. After meeting this demand, the HSSW produced a surplus of 13,460.99 kWh from a total generation of 60,575.8 kWh. This surplus electricity was offset through net metering. Using Eq. (2), the weighted average electricity rate was calculated by considering the seasonal distribution of the energy consumption (Table 11). Based on this rate, the resulting electricity cost savings from the surplus generation were calculated using Eq. (3). This analysis indicated that the elementary school building equipped with HSSWs achieved annual electricity cost savings of approximately 1.44 million KRW. Additional cost savings could also be realized if the basic charge were to be reduced.

$$Weightedaverageelectricityrate(KRW/kWh) = \sum\left(\frac{seasonalenergyconsumption}{totalenergyconsumption} \times electricityrate\right) \quad (2)$$

Table 11
Electricity rates and consumption data based on the monthly energy consumption.

Season	Energy consumption [kWh]	Consumption rate (%)	Electricity rate [KRW/kWh]	Weighted average electricity rate [KRW/kWh]
Winter	16,018.18	34.0	114.5	38.93
Spring & Fall	17,984.25	38.2	94.4	36.03
Summer	12,112.32	25.8	116.2	29.87
Total	47,114.80	100		107.26

$$\begin{aligned} Electricitysavings(\text{KRW/yr}) &= surpluspower \times totalweightedaverageelectricityrate \\ &= 13,460.99 \times 107.26 \\ &= 1,443,888\ \text{KRW/yr (VAT included)} \end{aligned} \quad (3)$$

4. Conclusions

This study analyzed the indoor environmental performance, energy consumption, and power generation of an elementary school equipped with an HSSW system using the simulation software DesignBuilder. The results confirmed the feasibility of ZEBs in South Korea and demonstrated the potential for energy prosumer applications. The key findings can be summarized as follows:

(1) The DF and average indoor illuminance were slightly higher for the HSSWs compared to the reference model (Low-E windows) due to their superior VLT, which was 8.9 % higher. However, at a distance of 3.5 m from the classroom window, the measured illuminance did not meet the classroom lighting standards, meaning that additional artificial lighting was necessary to ensure visual comfort.
(2) The indoor temperature was analyzed in terms of the solar heat gain. The annual solar heat gain for the HSSW was 36.46 % higher than that of the reference model. As a result, the indoor temperature increased by 0.7 to 1.3 °C with the HSSWs in both summer and winter. This rise in temperature was attributed to the higher SHGC and lower U-value of the HSSWs, which allowed more solar energy to enter and reduced thermal losses. These findings suggest that using HSSWs can reduce the heating demand, although it may slightly increase the cooling demand.
(3) The annual total energy consumption for the reference model was 1.66 % higher than that of the HSSWs. Heating energy consumption was higher for the Low-E windows as a result of the greater heat loss arising from their higher U-value, while the cooling energy consumption decreased due to the improved SHGC. However, lighting-energy consumption was higher for the reference model due to its lower VLT, which resulted in higher total energy consumption. Based on these results, HSSWs have the potential to reduce the heating load in cold climates, where buildings are more vulnerable to heat loss, thus increasing the energy savings.
(4) For the HSSWs, the annual total power generation was 60,576 kWh, which not only offset the building's annual total energy consumption but also produced a surplus of 13,461 kWh. This confirms the potential for the proposed window design to contribute to the establishment of ZEBs. By using the surplus electricity in the net metering system, building owners can reduce electricity costs associated with energy consumption. In particular, in the present study, the use of net metering led to estimated annual electricity cost savings of approximately 1.44 million KRW.

Overall, the lighting and thermal performance characteristics of HSSWs were analyzed in terms of the solar heat gain, indoor temperature, indoor illuminance, heating energy, cooling energy, lighting energy, and power generation. The results confirmed that HSSWs can reduce the annual total energy consumption compared to buildings using conventional Low-E windows, demonstrating that ZEBs are feasible. Furthermore, the potential for energy prosumer applications was verified through the utilization of surplus electricity.

In the future, to quantitatively evaluate the applicability and scalability of HSSWs, we plan to analyze performance variation between climate zones and different window-to-wall ratios. Additionally, sensitivity analyses will be conducted on key performance parameters for HSSWs (e.g., VLT and SHGC) to quantify the impact of design variables on indoor environmental conditions and energy performance. Furthermore, by integrating advanced power trading platforms such as virtual power plants, peer-to-peer energy trading, and energy storage systems, the model proposed in this study could be expanded into a full-scale energy prosumer system. This technological integration may offer a viable pathway to enhance both energy self-sufficiency and the economic performance of buildings. Nevertheless, based on the findings of this study, further technological advancements are required to improve the performance of HSSWs. Continued research is also necessary to evaluate the environmental and energy performance of BIPV systems across various building types and climate conditions. These efforts are crucial to realizing the potential of BIPV technologies for use in ZEBs and accelerating the transition toward a more sustainable built environment.

Declaration of generative AI and AI-assisted technologies in the writing process

During the preparation of this work, the authors used OpenAI's tool

ChatGPT in order to improve the readability and language. After using this tool, the authors carefully reviewed and edited the content as needed and take full responsibility for the content of the publication.

CRediT authorship contribution statement

Bo Rang Park: Writing – original draft, Funding acquisition. **A Young Kim:** Software. **Eun Ji Choi:** Data curation. **Yongseok Jun:** Conceptualization. **Jin Woo Moon:** Writing – review & editing, Funding acquisition.

Declaration of competing interest

The authors declare that they have no known competing financial interests or personal relationships that could have appeared to influence the work reported in this paper.

Acknowledgments

This research was supported by the Basic Science Research Program through the National Research Foundation of Korea (NRF) funded by the Ministry of Education (No.RS-2023-00237932), and an NRF grant funded by the Korean government (MSIT) (No. RS-2023-00217322).

Data availability

The authors do not have permission to share data.

References

[1] D.C. Law, Clean Energy DC Building Code Amendment Act of 2022. Council of the District of Columbia, 2022.

[2] California Air Resources Board, Zero-emission space and water heater standards, 2023.

[3] New York State, FY 2024 Budget highlights: Energy affordability, sustainable buildings, and clean energy. https://www.nyserda.ny.gov/About/Newsroom/2023-Announcements/2023-05-03-Governor-Hochul-Announces-FY-2024-Budget-Investments-in-Energy-Affordability, 2023.

[4] European Commission, Energy performance of buildings directive (EU/2024/1275), 2024.

[5] Net Zero News, https://www.netzeronews.kr/.

[6] Korea Energy Agency, Status of zero energy building certification grades. https://zeb.energy.or.kr/, 2024.

[7] Exactitude Consultancy, Solar power market by technology, application, solar module and region: Global trends and forecast from 2022 to 2029, 2023.

[8] S. Shi, N. Zhu, Challenges and optimization of building-integrated photovoltaics (BIPV) windows: a review, Sustainability 15 (22) (2023) 15876, https://doi.org/10.1016/j.icheatmasstransfer.2024.108056.

[9] M.H. Chung, B.R. Park, E.J. Choi, Y.J. Choi, C.Y. Lee, J.I. Hong, H.U. Cho, J.H. Cho, J.W. Moon, Performance level criteria for semi-transparent photovoltaic windows based on dye-sensitized solar cells, Sol. Energy Mater. Sol. Cells 217 (2022) 110683, https://doi.org/10.1016/j.solmat.2020.110683.

[10] J.H. Kim, S.H. Han, Energy generation performance of window-type dye-sensitized solar cells by color and transmittance, Sustainability 12 (21) (2020) 8961, https://doi.org/10.3390/su12218961.

[11] B.R. Park, T.W. Kim, J.Y. Hyun, J.W. Moon, Climate-zone-dependent applicability of semi-transparent cadmium-telluride-type solar cells as a building material with display characteristics, Energ. Build. 287 (2023) 112977, https://doi.org/10.1016/j.enbuild.2023.112977.

[12] A.K. Mohammad, A. Garrod, A. Ghosh, Do building-integrated photovoltaic (BIPV) windows propose a promising solution for the transition toward zero energy buildings? A review, J. Build. Eng. 79 (2023) 107950, https://doi.org/10.1016/j.jobe.2023.107950.

[13] J.Y. Hyun, B.R. Park, N.H. Kim, J.W. Moon, Building energy performance of DSSC BIPV windows in accordance with the lighting control methods and climate zones, Sol. Energy 244 (2022) 279–288, https://doi.org/10.1016/j.solener.2022.08.039.

[14] L. Chen, X. Zheng, J. Yang, J.H. Yoon, Impact of BIPV windows on building energy consumption in street canyons: model development and validation, Energ. Build. 249 (2021) 111207, https://doi.org/10.1016/j.enbuild.2021.111207.

[15] S. Yang, F. Fiorito, A. Sproul, D. Prasad, Optimising design parameters of a building-integrated photovoltaic double-skin façade in different climate zones in Australia, Buildings 13 (2023) 1096, https://doi.org/10.3390/buildings13041096.

[16] S. Yang, A. Cannavale, A. Di Carlo, D. Prasad, A. Sproul, F. Fiorito, Performance assessment of BIPV/T double-skin façade for various climate zones in Australia: effects on energy consumption, Sol. Energy 199 (2020) 377–399, https://doi.org/10.1016/j.solener.2020.02.044.

[17] S. Yang, F. Fiorito, D. Prasad, A. Sproul, A. Cannavale, A sensitivity analysis of design parameters of BIPV/T-DSF in relation to building energy and thermal comfort performances, J. Build. Eng. 41 (2021) 102426, https://doi.org/10.1016/j.jobe.2021.102426.

[18] H. Jhumka, S. Yang, C. Gorse, S. Wilkinson, R. Yang, B.J. He, D. Prasd, F. Fiorito, Assessing heat transfer characteristics of building envelope deployed BIPV and resultant building energy consumption in a tropical climate, Energ. Buildings 298 (2023) 113540, https://doi.org/10.1016/j.enbuild.2023.113540.

[19] F. Roberts, S. Yang, H. Du, R. Yang, Effect of semi-transparent a-Si PV glazing within double-skin façades on visual and energy performances under the UK climate condition, Renew. Energy 207 (2023) 601–610, https://doi.org/10.1016/j.renene.2023.03.023.

[20] C.J. Traverse, R. Pandey, M.C. Barr, R.R. Lunt, Emergence of highly transparent photovoltaics for distributed applications, Nat. Energy 2 (2017) 849–860. https://www.nature.com/articles/s41560-017-0016-9.

[21] DesignBuilder. https://designbuilder.co.uk, 2019.

[22] Ministry of Trade, Industry and Energy & Korea Energy Agency New and Renewable Energy Center, Mandatory installation of renewable energy facilities in public institutions. https://www.knrec.or.kr, 2024.

[23] Zero Energy Building. http://www.zeroenergy.kr, 2024.

[24] Ministry of Education & Korean Educational Development Institute, 2023 statistical yearbook of education, 3-31 Quantity of Energy Usage, 2023.

[25] D.G. Hwang, A study on the improvement of standard models and unit loads by non-residential building types, University of Seoul, 2019. Ph.D. Dissertation.

[26] Korea Institute of Civil Engineering and Building Technology, Establishment of standard model database for greenhouse gas reduction potential analysis in the building sector (2), 2017.

[27] Architecture HUB. https://www.hub.go.kr/portal/, 2024.

[28] ASHRAE, ASHRAE guideline 14-2014: Measurement of energy, demand, and water savings, 2014.

[29] ASHRAE, ASHRAE guideline 14-2023: Measurement of energy, demand, and water savings, 2023.

[30] J.H. Kim, et al., Energy generation performance of window-type dye-sensitized solar cells by color and transmittance, Sustainability 12 (2020) 8961, https://doi.org/10.3390/su12218961.

[31] R. Perez, P. Ineichen, R. Seals, J. Michalsky, R. Stewart, Modeling daylight availability and irradiance components from direct and global irradiance, Sol. Energy 44 (1990) 271–289, https://doi.org/10.1016/0038-092X(90)90055-H.

[32] Korea Electric Power Corporation. https://online.kepco.co.kr/, 2025.